catalysts

MDPI

Article

The Impact of CeO_2 Loading on the Activity and Stability of PdO/γ-AlOOH/γ-Al_2O_3 Monolith Catalysts for CH_4 Oxidation

Hamad AlMohamadi [1,2] and Kevin J. Smith [1,*]

1 Department of Chemical and Biological Engineering, University of British Columbia, 2360 East Mall, Vancouver, BC V6T 1Z3, Canada; mohamahh@chbe.ubc.ca
2 Faculty of Engineering, Islamic University of Madinah, Madinah 41455, Saudi Arabia
* Correspondence: kjs@mail.ubc.ca; Tel.: +1-604-822-3601; Fax: +1-604-822-6003

Received: 3 May 2019; Accepted: 14 June 2019; Published: 21 June 2019

Abstract: This study reports on the activity and stability of PdO/γ-AlOOH/γ-Al_2O_3 monolith catalysts, promoted with varying amounts of CeO_2, for CH_4 oxidation. Although the beneficial effects of CeO_2 have been reported for powdered catalysts, this study used a cordierite ($2MgO.2Al_2O_3.5SiO_2$) mini-monolith (400 cells per square inch, 1 cm diameter × 2.5 cm length; ~52 cells), washcoated with a suspension of γ-Al_2O_3 combined with boehmite (γ-AlOOH), followed by sequential deposition of Ce and Pd (0.5 wt.%) by wetness impregnation. The monolith catalysts' CH_4 oxidation activity and stability were assessed in the presence of CO, CO_2, H_2O and SO_2 at low temperature (≤550 °C), relevant to emission control from lean-burn natural gas vehicles (NGVs). The CeO_2 loading (0 to 4 wt.%) did not significantly impact the adhesion and thermal stability of the washcoat, but CeO_2 reduced the inhibition of CH_4 oxidation by H_2O and SO_2. The catalyst activity, measured by temperature-programmed methane oxidation (TPO) in a dry feed gas with 0.07 vol.% CH_4, showed that adding CeO_2 to the γ-AlOOH/γ-Al_2O_3 washcoat suppressed the activity of the catalysts; whereas, CeO_2 improved the catalyst activity when H_2O (2 and 5 vol.%) was present in the feed gas. Moreover, adding CeO_2 decreased catalyst deactivation that occurred in the presence of 10 vol.% H_2O and 5 ppmv SO_2 at 500 °C, measured over a 25 h time-on-stream (TOS) period. The highest catalyst activity and stability for CH_4 oxidation in the presence of H_2O was obtained by adding 2 wt.% CeO_2 to the washcoat.

Keywords: natural gas vehicle; exhaust gas; methane; oxidation; catalyst; monolith

1. Introduction

Natural gas is considered to be a suitable alternative fuel because combustion of natural gas produces less greenhouse gas (GHG) emissions per unit of energy than gasoline or diesel. The lower emissions are due to the high hydrogen-to-carbon ratio of the main component of natural gas, CH_4 [1]. Use of natural gas as a vehicle fuel is growing at about 21% per year worldwide. However, unburned CH_4 emitted in the exhaust gas of natural gas vehicles (NGVs), limit their growth [2,3] and several studies have focused on improving the efficiency of the NGV catalytic convertor so as to reduce CH_4 emissions to an acceptable level [1,4–11]. Oxidation of CH_4 from NGV emissions is difficult because of the low concentrations of CH_4 (400–1500 ppm), the low exhaust gas temperatures (150–550 °C) from lean-burn NGVs [2,10] and the presence of high concentrations of H_2O (5–15 vol.%) and CO_2 (10 vol.%) [3].

Although Pd is known to be the most active metal catalyst for CH_4 oxidation at low temperature [12–14], the support (Al_2O_3, CeO_2, ZrO_3, TiO_2, TaO_3) also has an impact on the catalyst

activity [15]. Haneda et al. [16] investigated two catalysts: (i) a Pd/CeO_2-Al_2O_3 that had been reduced in flowing H_2 at 900 °C prior to impregnation with Pd nitrate and (ii) a Pd/Al_2O_3 catalyst. They reported that the Pd/CeO_2-Al_2O_3 was more active than the Pd/Al_2O_3 at 350°C. Park et al. [17] have also stated that Pd/ZrO_2 is more active and stable than the Pd/γ-Al_2O_3 when hydrothermally aged at 600 °C for 100 h. One of the more active CH_4 oxidation catalysts reported recently encapsulated PdO in porous CeO_2 [6], ensuring a strong interaction between the CeO_2 and the PdO, combined with a high O exchange capacity of CeO_2. The effect of CeO_2 and the optimum loading varies in different studies, depending on the catalyst preparation method and the contact between the CeO_2 and PdO, [18,19], although high loadings of Ce (50 wt.%) are known to suppress catalytic activity [19]. Ramírez et al. [19] reported that increasing the amount of Ce (2 to 50 wt.%) added to Pd/Al_2O_3 catalysts, decreased the CH_4 oxidation activity, measured in a dry feed gas with 0.5 vol.% CH_4 and 1 vol.% O_2. Stasinska et al. [20] reported enhanced activity of a sol-gel prepared PdO/Ce-Al_2O_3 catalyst, compared to PdO/Al_2O_3, when operated at low temperature (<427 °C). In contrast, Groppi et al. [21] reported that the activity of a Pd/Al_2O_3 catalyst for CH_4 combustion was not affected by the CeO_2 except at high temperature. Fan et al. [22] studied the effect of adding Ce to Pt-Pd/Al_2O_3 catalysts for CH_4 oxidation and reported that adding 0.6 wt.% Ce improved the activity and the stability of the Pt-Pd/Al_2O_3 catalyst [22] by preventing the growth of PdO particles [22]. Persson et al. [23] studied the effect of Al_2O_3, ZrO_2, $LaMnAl_{11}O_{19}$, and Ce-ZrO_2 washcoats applied to cordierite monoliths, on the activity of Pd-Pt catalysts for CH_4 oxidation. The initial CH_4 oxidation activity was measured at atmospheric pressure in 1.5 vol.% CH_4 in dry air and a space velocity of 250,000 h^{-1}. They reported that at low temperature (470 °C), Pd-Pt/Al_2O_3 was the most active catalyst while the Pd-Pt/Ce-ZrO_2 catalyst was the most active at high temperatures (620–800°C). The high surface area of the Al_2O_3 (90 m^2/g) compared to the Ce-ZrO_2 (10 m^2/g) accounted for the higher activity at low temperature [23,24]. Also, the authors stated that Ce-ZrO_2 improved the stability of the PdO because Ce-ZrO_2 re-oxidized Pd^0 to PdO faster than Al_2O_3 [23]. Recent studies of CH_4 oxidation at low temperature have also shown that PdO sites on Pd-O-Ce surfaces have high activity [6,25].

Although Pd catalysts have high initial activity, they deactivate upon exposure to the exhaust gas (CH_4, CO, CO_2, SO_x, NO_x and H_2O) for long periods [5,26], Pd being very sensitive to sulfur and H_2O which play a major role in inhibiting catalyst activity [27,28]. Alyani and Smith [29] studied the effect of adding CeO_2 to Pd/γ-Al_2O_3 for CH_4 oxidation on powder catalysts and reported that Pd/γ-Al_2O_3 was more active than Pd/Ce/γ-Al_2O_3 in a dry CH_4/O_2 gas environment. However, Pd/Ce/γ-Al_2O_3 was more stable in the presence of H_2O because adding Ce reduced the inhibition effect of H_2O on CH_4 oxidation [29]. Moreover, Gomathi et al. [30] prepared Pd/CeO_2 nanostructured catalysts using a new technique of surface-assisted reduction. These catalysts were shown to be very active for CH_4 oxidation with T_{50}, the temperature at which 50% conversion occurs, of <300 °C. The catalysts had higher stability than Pd/γ-Al_2O_3 in the presence of H_2O [30]. Toso et al. [31] reported the effect of H_2O on CH_4 oxidation over a series of Pd/CeO_2-SiO_2 powdered catalysts. The stability of the catalysts, measured in the presence of 5 vol.% H_2O, 0.5 vol.% CH_4 and 2 vol.% O_2 at 450 °C, increased with increased Ce content because accumulation of hydroxyl groups decreased, which improved O_2 exchange and hence improved the stability of the catalysts [31].

Conventional catalytic converters are prepared by applying a high surface area washcoat layer to a cordierite ceramic monolith, [32–34] with the active metal subsequently dispersed on the washcoat support. Current commercial catalysts for CH_4 oxidation show a high activity at low temperature, however, they are less active and unstable in the presence of H_2O [35–38] and SO_2 [39]. The inhibition of CH_4 oxidation by water on Pd catalysts has been extensively investigated [2,10,11,24,26,28,35,40–43]. $Pd(OH)_2$ formation and accumulation on the surface of the catalyst are proposed reasons for the inhibition of the catalyst activity [24,28]. Water adsorption on the active site also plays a major role in inhibiting the catalyst activity [33,44–46].

γ-Al_2O_3 is commonly used as the washcoat of ceramic monoliths [47], providing a high surface area support on which to disperse the active phase [48,49]. One of the drawbacks of γ-Al_2O_3 is

a low thermal stability at high temperature in the presence of water [50]. CeO_2 has been used in TWCs because of its ability to store O_2 under lean operating conditions and release O_2 under fuel rich operating conditions [51–53]. Ozawa and Kimura [54] reported that the thermal stability of γ-Al_2O_3 was enhanced by the addition of CeO_2. Piras et al. [55] proposed that $CeAlO_3$ formation improved thermal stability of γ-Al_2O_3 because $CeAlO_3$ impedes the growth of α-Al_2O_3 crystals. Pingping et al. [56] reported an improved thermal stability of a γ-Al_2O_3 washcoat mixed with CeO_2–ZrO_2–La_2O_3 [56].

The above literature provides significant evidence from studies of powdered catalysts that Ce improves the activity and the stability of Pd catalysts for CH_4 oxidation in the presence of H_2O. For monolith catalysts, the effect of Ce has been reported mostly at high temperatures in dry feed gas, conditions that are relevant to emissions from gasoline engines. The present study is focused on the impact of Ce addition to Pd catalysts supported on γ-Al_2O_3/AlOOH washcoated cordierite monoliths (400 cells per square inch (CPI); 1 cm diameter × 2.54 cm length). The monolith catalysts have been assessed at high space velocity and at temperatures ≤550 °C in the presence of CO, CO_2, H_2O and SO_2 to closely mimic the exhaust gas from lean-burn NGVs. The objective of the study was to determine the impact of Ce on the adhesion and stability of the washcoat, and to determine the CH_4 oxidation activity and stability of the Pd/CeO_2/γ-AlOOH/γ-Al_2O_3 catalysts operated in the presence of H_2O, CO, CO_2 and SO_2. The Ce loading that provided the highest activity and stability of the monolith catalyst was also determined.

2. Results

2.1. Monolith Characterization

Figure 1 shows the effect of the Ce loading on the adhesion properties and thermal stability of the applied washcoat. The catalysts have very similar adhesion as reflected in the total weight loss of 1–2 wt.% following the vibration test, even though the samples with CeO_2 were calcined twice at 450 °C for 15 h. The thermal stability of the washcoat was not significantly influenced by adding CeO_2 either, as indicated by the similar weight loss among all samples recorded after the second vibration test that followed the high temperature treatment (1000 °C for 7 h). Hence, we conclude that the addition of the CeO_2 does not have a significant impact on the adhesion and thermal stability of the washcoat when applied to the cordierite monolith.

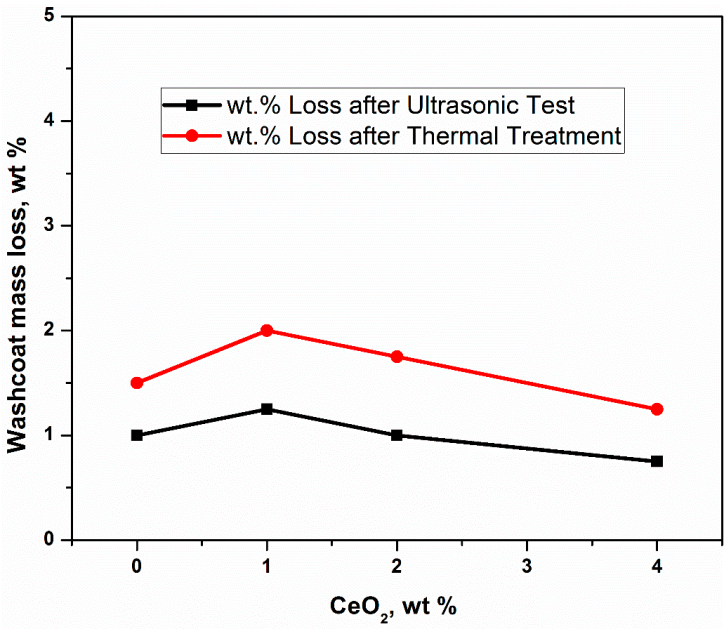

Figure 1. Effect of CeO_2 loading on the adhesion properties and thermal stability of the washcoat.

Table 1 reports the textural properties of the monolith catalysts prepared in this study with varying amounts of CeO_2. For the Pd0Ce catalyst without CeO_2 in the washcoat, the surface area was 55 m^2/g. As the CeO_2 content of the catalyst increased, the surface area decreased to 46 m^2/g for the catalyst with 4 wt.% Ce (Pd4Ce). Moreover, the pore volume decreased with increased CeO_2 loading. For the Pd0Ce-used catalyst analyzed after both the TPO and TOS tests, the surface area decreased marginally to 45 m^2/g, while it decreased to 42 m^2/g for the Pd2Ce-used catalyst.

Table 1. Textural properties and CO uptake of $PdO/CeO_2/\gamma$-$AlOOH/\gamma$-Al_2O_3 monolith catalysts with varying Ce content.

Sample	Ce Content	BET Area	Pore Volume	Average Pore Diameter	CO Uptake
	wt.%	m^2/g	cm^3/g	nm	µmol/gcat
Pd0Ce	0	55	0.24	9	19.4
Pd1Ce	1	51	0.17	13	13.5
Pd2Ce	2	49	0.14	11	11.5
Pd4Ce	4	46	0.12	10	8.5
Pd0Ce—used	0	45	0.12	10	10
Pd2Ce—used	2	42	0.11	10	8.8

CO chemisorption analysis was done after reduction of both the fresh and used Pd0Ce and Pd2Ce catalysts (Table 1). The fresh Pd0Ce (no CeO_2 in the catalyst) had a higher CO uptake than Pd2Ce (2 wt.% CeO_2 in the catalyst) and generally the CO uptake decreased as the CeO_2 loading increased. However, the CO uptake for the used Pd0Ce decreased significantly (from 19.4 µmol/gcat to 10 µmol/gcat); whereas, for Pd2Ce the loss in CO uptake was much less significant (from 11.5 µmol/gcat to 8.8 µmol/gcat).

SEM images of monolith sections of the Pd0Ce (no CeO_2) and Pd2Ce (2 wt.% CeO_2) catalysts are compared in Figure 2A–D. Differences in thermal expansion between cordierite and alumina creates minor cracks on the washcoat surface of both catalysts [4]. Figure 3 shows the SEM-EDX analysis of the monolith x-section, indicating a uniform dispersion of the Al, Ce and Pd in the channels of the Pd1Ce catalyst. The EDX analysis was done at different locations of each catalyst and Table 2 reports the average and standard deviation of the analyses. Note that the EDX analysis results do not include the cordierite because of the sampling depth (a few microns) of the method. Accounting for the mass of cordierite (73 wt.%), the Pd data of Table 2 are in very good agreement with the Pd nominal composition (1.8 wt %). However, the Ce content is lower than the nominal composition (Table 1 data divided by 0.27), suggesting a greater penetration depth of Ce within the washcoat, in part because Ce was added in the first impregnation.

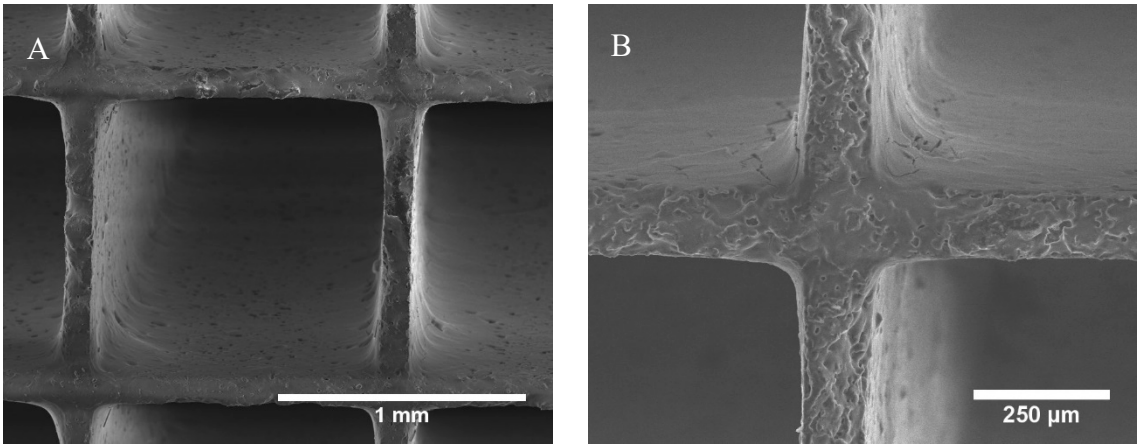

Figure 2. *Cont.*

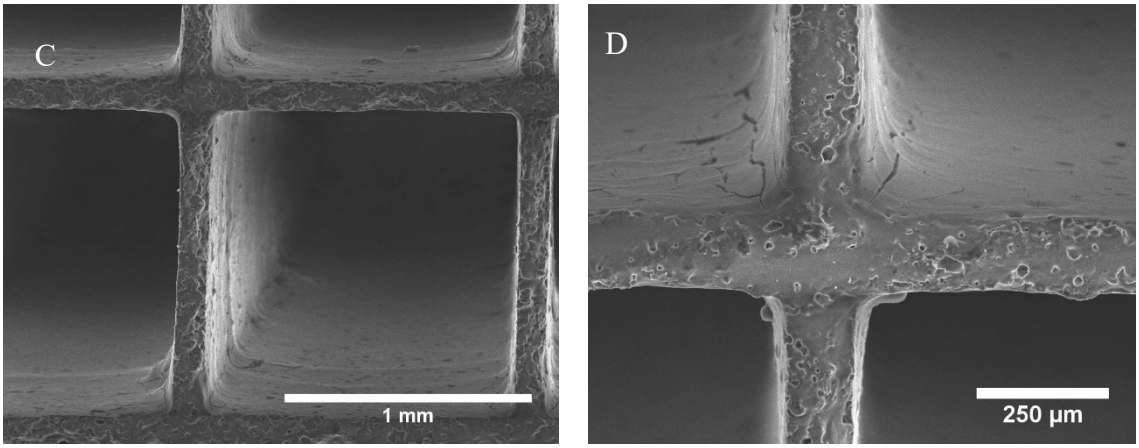

Figure 2. SEM images of the monolith catalysts Pd0Ce (**A**,**B**) and Pd2Ce, (**C**,**D**).

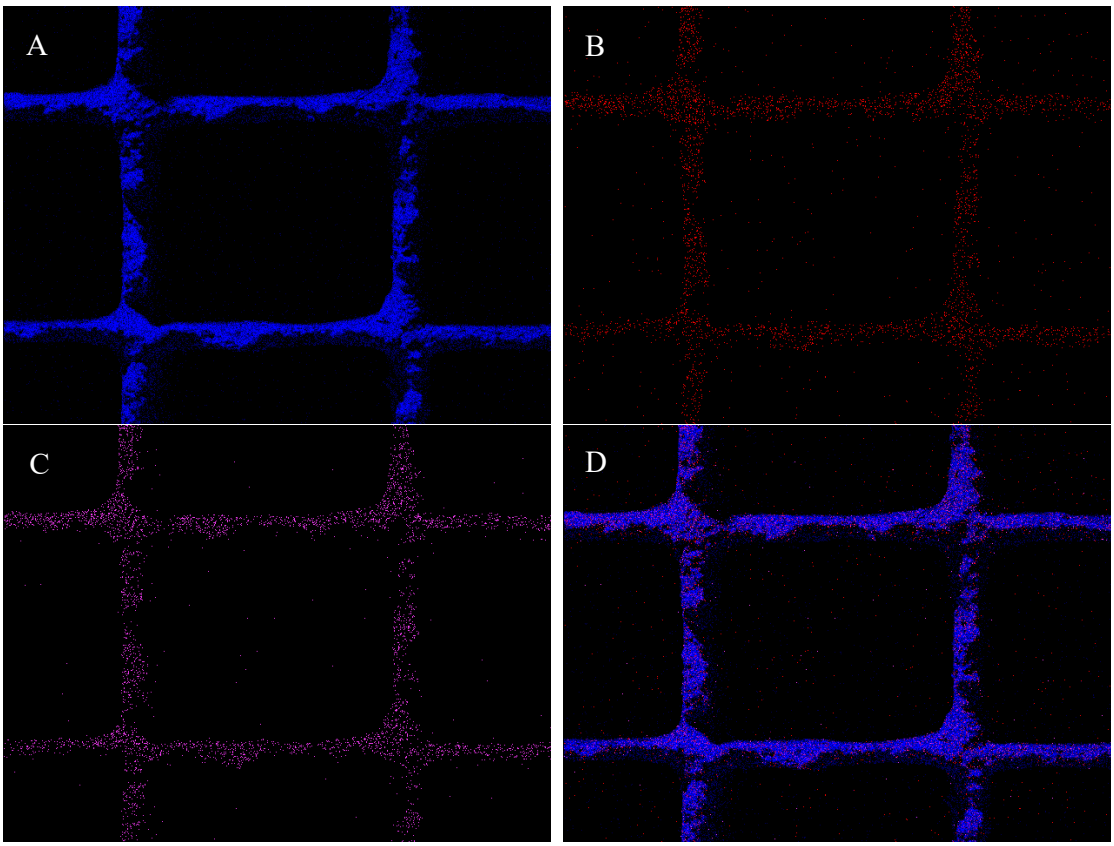

Figure 3. SEM-EDX analysis of Pd1Ce catalyst: (**A**) Al, (**B**) Ce, (**C**) Pd, and (**D**) Pd-Ce-Al.

Table 2. EDX elemental analysis of the monolith catalysts.

	O, wt.%	Al, wt.%	Ce, wt.%	Pd, wt.%
Pd0Ce	53.2 ± 1	45.1 ± 2.1	0	1.7 ± 0.2
Pd1Ce	50.1 ± 1.9	45.2 ± 2.4	3.2 ± 0.8	1.5 ± 0.4
Pd2Ce	48.2 ± 1.6	44.3 ± 2.1	5.9 ± 0.7	1.6 ± 0.3
Pd4Ce	45.9 ± 1.9	41.1 ± 1.5	11.3 ± 0.5	1.7 ± 0.2

Table 3 presents the Pd $3d_{5/2}$ and $3d_{3/2}$ binding energies (B.E.s), the Pd, Al and O surface compositions and the Pd/Al ratio for all the catalysts, as measured by XPS. The data show that as the loading of Ce increased, the concentration of Pd on the surface increased, as did the Pd/Al ratio. Figure

S1 shows the XPS Pd 3d spectral analysis for all the samples. For Pd2Ce the Pd $3d_{5/2}$ B.E was 337.1 eV, higher than for Pd0Ce (336.6 eV). Figure S2 shows the Pd 3d XPS data for the fresh and used Pd0Ce catalyst and the fresh and used Pd2Ce catalyst. The Pd $3d_{5/2}$ B.E increased by 0.3 eV for Pd0Ce and by 0.6 eV for Pd2Ce after use. Furthermore, the surface Pd/Al ratio decreased after use for both catalysts. From the fresh and used B.E. data, it can be concluded that the Pd surface was in an oxidized state [57] and the decrease in the Pd/Al ratio after use is due to catalyst aging, as has been reported previously for powdered catalysts that operated under similar conditions [29,58].

Table 3. XPS analysis of PdO/CeO_2/γ-AlOOH/γ-Al_2O_3 monolith catalysts with varying Ce content.

Monolith Catalyst	Pd B.E.		Surface Composition				
	$3d_{5/2}$	$3d_{3/2}$	Pd	Ce	Al	O	Pd/Al
	eV	eV	atom %				%
Pd0Ce	336.6	342.1	0.2	0	39.1	60.7	0.51
Pd1Ce	337.1	342.3	0.28	0.29	35.13	64.3	0.80
Pd2Ce	337.1	342.3	0.30	0.45	31.25	68	0.96
Pd4Ce	336.9	342.1	0.69	0.51	35.4	63.4	1.95
Pd0Ce-Used	336.9	342.2	0.17	0	37.5	62.3	0.45
Pd2Ce-Used	337.7	342.9	0.26	0.64	35.7	63.4	0.73

2.2. Catalysts Activity and Stability

The activities of the monolith catalysts, measured by TPO, are reported in Figure 4 and the T_{50} temperatures (the temperature required for 50% CH_4 conversion) are summarized in Table 4. In dry feed gas (i.e., no H_2O in the feed gas), all the catalysts reached approximately 100% CH_4 conversion at 450 °C. TPO analysis of the catalysts without water in the feed gas yield T_{50} of ≤362 °C for all the catalysts, as shown in Table 4. With H_2O added to the feed gas, the light-off curves shifted to higher temperatures for all catalysts, reflecting the loss in catalyst activity in the presence of H_2O. Addition of CeO_2 to the washcoat decreased the catalyst activity when measured in the dry feed gas; whereas, when H_2O (2 and 5 vol.%) was present in the feed, the CeO_2 improved the catalyst activity relative to the catalyst without CeO_2 (Pd0Ce), as shown in Figure 4B,C. From the results in Table 4 and Figure 4 it can be concluded that the Pd2Ce (2 wt.% Ce) catalyst had the highest catalytic activity in the presence of H_2O in the feed gas.

Table 4. Temperature-programmed oxidation T_{50} conversion for the catalysts in dry and wet feed gas. [Reaction conditions: GHSV = 36,000 h^{-1}, Feed composition: 0.07 vol.% CH_4, 8.5 vol.% O_2, 0.06 vol.% CO, 8 vol.% CO_2 and 0, 2 or 5 vol.% H_2O in N_2 and He.].

Monolith	T_{50} Dry Gas	T_{50} Wet Gas 2 vol.% H_2O	T_{50} Wet Gas 5 vol.% H_2O
Pd0Ce	317	379	401
Pd1Ce	322	370	385
Pd2Ce	333	352	370
Pd4Ce	362	377	390

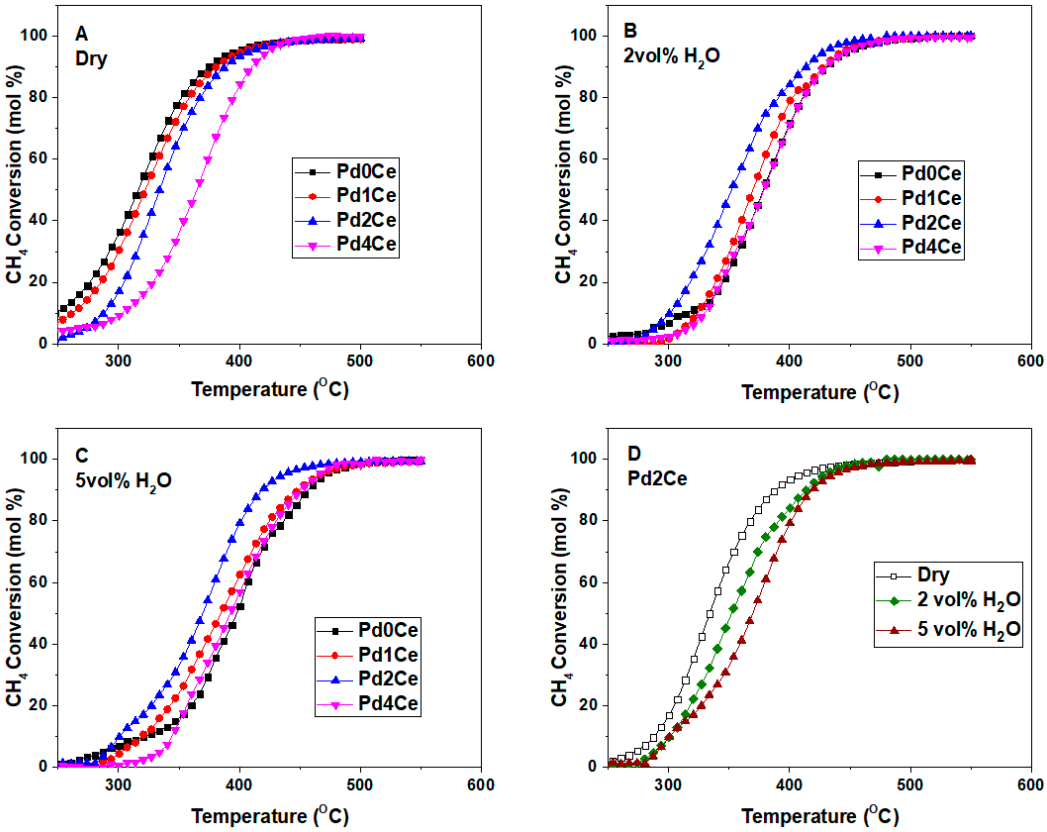

Figure 4. Temperature-programmed CH_4 oxidation profile showing the initial activity of the catalysts as a function of temperature. Reaction conditions: GHSV of 36,000 h^{-1}, Feed gas composition: 0.07 vol.% CH_4, 8.5 vol.% O_2, 0.06 vol.% CO, 8 vol.% CO_2 and 0, 2 or 5 vol.% H_2O in N_2 and He. (**A**) Dry feed 0 vol.% H_2O; (**B**) Wet feed 2 vol.% H_2O; (**C**) Wet feed 5 vol.% H_2O; (**D**) Initial activity of Pd2Ce catalyst.

The results of the time-on-stream (TOS) experiments with 10 vol.% H_2O in the feed at 425 °C and 550 °C are shown in Figure 5A and Figure S3, respectively. For all the catalysts, Figure 5A shows that at the lower reaction temperature, the CH_4 conversion decreased with the addition of H_2O to the reactor feed gas. The Pd0Ce (no CeO_2) catalyst deactivated very rapidly with the conversion of CH_4 decreasing to 60% within 2 h and after 7 h the conversion decreased to 50%. After the H_2O was removed from the feed gas, the conversion recovered to 58%. The Pd2Ce was the most stable catalyst in the presence of 10 vol.% H_2O at 425 °C. The conversion decreased to 70% in 7 h and recovered to 80% after the H_2O was removed. At 550 °C all the catalysts showed good stability in the presence of 10% H_2O (Figure S3). Figure 5B shows, however, that in the presence of both 10% H_2O and 5 ppmv SO_2, the catalyst deactivation was severe, although the catalyst with the CeO_2 (Pd2Ce) deactivated more slowly and reached a slightly higher conversion after 20 h than the catalyst without CeO_2 (Pd0Ce).

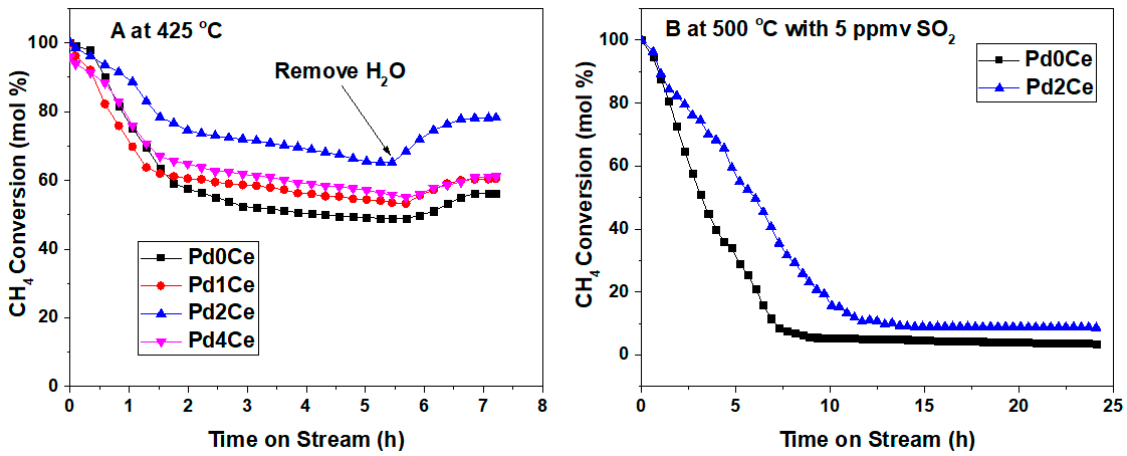

Figure 5. TOS results after adding: (**A**) 10 vol.% H_2O added to the dry feed gas at 425 °C and (**B**) 10 vol.% H_2O and 5 ppmv SO_2 added to the dry feed gas at 500 °C. Reaction conditions: GHSV = 36,000 h^{-1}, Feed gas composition: 0.07 vol.% CH_4, 8.5 vol.% O_2, 0.06 vol.% CO, 8 vol.% CO_2 in N_2 and He.

After the TOS experiments in H_2O the catalysts were purged using N_2 at 120 °C for 12 h and then re-assessed by TPO in dry feed gas. The results illustrate that the Pd2Ce catalyst had the highest activity among all the used catalysts, as shown in Figure 6. The T_{50} for the Pd2Ce catalyst increased from 333 °C for the fresh catalyst to 350 °C for the used sample, an increase of 17 °C. In contrast, for the Pd0Ce catalyst T_{50} increased by 45 °C. Hence, we conclude from both the TPO and TOS results that the addition of 2 wt.% CeO_2 to the catalyst/washcoat improved the stability and the activity of the monolith catalyst for CH_4 oxidation in the presence of H_2O in the feed gas. In the presence of H_2O and SO_2 the benefit of CeO_2 remains, but is less pronounced.

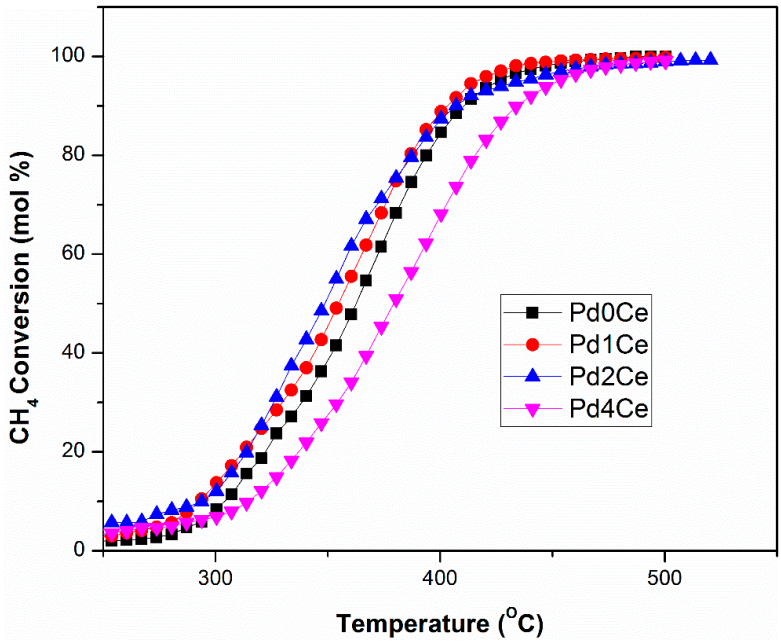

Figure 6. Temperature-programmed CH_4 oxidation profile: the initial activity of the catalysts as a function of temperature after the catalysts were regenerated. Reaction conditions: GHSV = 36,000 h^{-1}, Feed gas composition: 0.07 vol.% CH_4, 8.5 vol.% O_2, 0.06 vol.% CO and 8 vol.% CO_2 in N_2 and He.

The CO oxidation was measured to quantify the activity of the catalyst for CO oxidation with and without CeO_2 in the washcoat. The results show that adding CeO_2 did not have a significant impact on the activity of the catalysts for CO oxidation and all catalysts reached 100% CO conversion

at temperature <220 °C, as reported in Figure S4. Also, CO conversion, measured during the TOS test reached 100% for all the catalysts at 425 °C and 550 °C.

3. Discussion

The BET surface area and the pore volume of the catalysts decreased with increased CeO_2 loading, in agreement with results in the literature [19,29,59]. With increased CeO_2 loading, the Al_2O_3 pores were filled by CeO_2, leading to a decrease in the surface area and the pore volume [18,60,61]. For both Pd0Ce and Pd2Ce, the BET surface area and the pore volume decreased after the TPO and TOS experiments, which likely resulted from some sintering of the washcoat [4].

The CO chemisorption results showed that CeO_2 loading had an impact on the CO uptake. The CO uptake for Pd0Ce (0 wt.% Ce) and Pd4Ce (4 wt.% Ce) was 19.4 μmol/gcat and 8.5 μmol/gcat, respectively, although they had the same Pd loading. A similar loss in CO uptake in the presence of CeO_2 has been noted previously [29,59]. The catalysts were reduced in H_2 for 1 h at 100 °C before measuring the CO uptake. The decrease in the CO uptake with increased CeO_2 loading is a consequence of a decrease in the reduction of PdO to Pd in H_2 prior to the CO uptake measurement, caused by the presence of CeO_2 [19,62]. Yao et al. [63] and Oh et al. [64] reported that adding CeO_2 to Pd/Al_2O_3 stabilized the PdO, making it difficult to reduce. Xiao et al. [65] reported the absence of Pd^0 in the XPS spectra of a 2 wt.%Pd/CeO_2 catalyst after reduction in H_2 for 1 h at 300 °C and concluded that Pd was present only as PdO because of a strong interaction between Pd and Ce that suppressed the reduction of the PdO. The decrease in CO uptake for Pd0Ce and Pd2Ce following their use, results from a loss in active surface sites after exposure to high amounts of H_2O at 425 °C and 550 °C for 14 h [66].

After the catalysts were calcined at 450 °C for 15 h in air flow, the Pd was present as PdO [10,41,67], confirmed by the $Pd_{5/2}$ B.E. of 336.6 ± 0.3 eV (Table 3). The $Pd_{5/2}$ B.E. increased by 0.5 eV and the surface Pd/Al ratio increased with 1 and 2 wt.% CeO_2. Adding CeO_2 leads to a marginal increase in the binding energy of Pd $3d_{5/2}$ due to charge transfer from CeO_2 to PdO [29,68]. The binding energy of the Pd $3d_{5/2}$ for catalysts Pd0Ce and Pd2Ce also increased after exposure to 10 vol.% H_2O at 425 °C for 7 h and 550 °C for 7 h, ascribed to the reconstruction of Pd species [65]. In the study by Shyu et al. [68] Pd 3d spectra of 0.6%Pd/CeO_2 and 6.8%Pd/Al_2O_3 catalysts were compared. After the catalysts were calcined at 800 °C a peak at 337 eV, corresponding to PdO was observed for both catalysts. The catalysts were subsequently reduced at 920 °C and exposed to ambient air, whereupon a peak at 337.0 eV was observed for the 0.6%Pd/CeO_2 catalyst but not the 6.8%Pd/Al_2O_3, confirming that CeO_2 increased the oxidation state of Pd.

Even though adding 1–4 wt.% CeO_2 to Pd/Al_2O_3 increased the surface Pd/Al ratio (i.e., Pd dispersion), the TPO data using a dry feed gas showed that adding CeO_2 decreased the activity of the catalyst, consistent with several previous studies [63,64,68]. Oh et al. [64] reported that the activity of Pd/Al_2O_3 and Pt/Al_2O_3 catalysts decreased with the addition of CeO_2 and suggested this was due to a strong interaction between the CeO_2 and the Pd that led to highly oxidized but less active PdO catalysts [64,68]. In this study, the results of CO uptake and TPO in dry feed gas suggest a decrease in the activity of the catalyst resulting from a strong interaction between CeO_2 and Pd that retains PdO species on the catalyst surface.

Ciuparu et al. [24] reported that the oxygen exchange between the support of the catalyst and Pd-vacancies is interrupted by H_2O adsorption on the support. Colussi et al. [69] showed that adding CeO_2 to Pd/Al_2O_3 improved oxygen exchange capacity of the catalyst, which enhanced Pd re-oxidation. Thus, the deactivation of Pd/Al_2O_3 by H_2O could be minimized by adding CeO_2 to Al_2O_3 since CeO_2 has a high oxygen exchange capacity. Yao et al. [51] also reported that the thermal stability of Al_2O_3 is improved by adding CeO_2 to Al_2O_3. The TPO data from the present study using a wet feed gas (2 vol.% H_2O) shows that the Pd2Ce catalyst had the highest activity with T_{50} of 372 °C. The activity in the presence of 2 vol.% H_2O decreased in order: Pd2Ce (2 wt.% Ce) > Pd1Ce (1 wt.% Ce) > Pd4Ce (4 wt.% Ce) > Pd0Ce (0 wt.% Ce). The same trend was obtained in the presence of 5 vol.% H_2O. For the Pd0Ce catalyst, T_{50} increased from 317 °C (dry feed gas) to 401 °C in a wet feed gas with 5 vol.% H_2O,

an increase of 84 °C. Although the Pd4Ce catalyst was the least active among the catalysts tested in dry or wet feed gas, adding CeO_2 reduced the T_{50} increase to 28 °C in the presence of 5 vol.% H_2O in the feed. A similar reduction in activity loss in the presence of water was observed for the Pd1Ce and Pd2Ce catalysts. Hence, we conclude that adding CeO_2 improved the activity of the catalysts in the presence of H_2O in the feed gas. In agreement with literature results, we assume that the higher oxygen exchange capacity of CeO_2 (compared to the γ-AlOOH/γ-Al_2O_3 washcoat) enhances oxygen exchange between the support and Pd vacancies, thereby enhancing re-oxidation of the Pd which in turn enhances the CH_4 oxidation rate observed in the presence of a wet feed gas.

Some studies report that Pd catalysts used for CH_4 oxidation deactivate in the presence of H_2O at low temperature (<500 °C) as a result of $Pd(OH)_2$ formation, [44,45,70] even though $Pd(OH)_2$ is formed at low temperatures <250 °C in the presence of H_2O and decomposes above 250°C [45]. Moreover, PdO is favored thermodynamically over $Pd(OH)_2$ and Pd^0 at the chosen operating conditions. In the present study, there was no evidence of Pd^0 (335.6 eV) nor $Pd(OH)_2$ (338.5 eV) from the XPS analysis. Pd was present as PdO in both the fresh and used catalysts, in agreement with the literature [29,43,58].

The adsorption of H_2O on the active sites of PdO also leads to an inhibition of the Pd catalysts for CH_4 oxidation [3,62]. Moreover, the nature of support for the catalyst has an impact on the activity and stability of CH_4 oxidation catalysts in the presence of H_2O [2,3,71–73]. A support with high hydrophobicity plays a role in reducing the adsorption of H_2O on the surface of the catalysts [71–73]. Carchini et al. [74] investigated H_2O adsorption and hydrophilicity of CeO_2 and Al_2O_3, and reported that Al_2O_3 had a higher affinity for H_2O than CeO_2, the latter being more hydrophobic. Thus, adding CeO_2 to the γ-AlOOH/γ-Al_2O_3 washcoat likely also increased the hydrophobicity of the washcoat and thereby reduced the adsorption of H_2O [31]. The TOS results of the present study at 550 °C in the presence of 10 vol.% H_2O in the feed (Figure S3), showed that the temperature plays a major role in the deactivation of the catalysts since all the catalysts showed high stability at 550 °C. The inhibition effect of H_2O decreased with increased temperature [2,40,45], consistent with the competitive adsorption kinetic model reported previously [29]. The TOS results from the present study show that at low temperature (425 °C), the deactivation in the presence of 10 vol.% H_2O is very significant. For the Pd0Ce catalyst the conversion of CH_4 decreased to 50% and recovered to 60% after the H_2O was removed from the feed gas. For the Pd2Ce catalyst with 2 wt.% Ce the conversion at 425 °C dropped to 70% and recovered to 80% after the H_2O was removed from the feed. The TOS results are in agreement with the TPO results for the wet feed. From the TOS and TPO results it can be concluded that adding 2 wt.% CeO_2 to the washcoat enhanced the activity and the stability of the Pd/γ-AlOOH/γ-Al_2O_3 catalyst in the presence of H_2O, suggesting that adding CeO_2 accelerates the Pd re-oxidation, which enhances the catalyst's activity when using a wet feed gas. Furthermore, an increase in the hydrophobicity of the washcoat leads to a decrease in H_2O adsorption on the surface of the washcoat, and hence higher activity. The results on the monolith catalysts reported herein are in good agreement with results using powdered catalysts [29–31].

Finally, the data of Figure 5B show that in the presence of H_2O and SO_2, severe deactivation occurs, but the presence of CeO_2 mitigates this behavior, albeit to a small degree. Ordonez et al. [39] reported similar effects on a powdered Pd/Al_2O_3 catalyst that was shown to be due to the formation of $PdSO_4$. The formation of $Al_2(SO_4)_3$ can also occur [9,75], resulting in changed textural properties that contribute to the loss in catalyst activity. In the presence of CeO_2, we expect that the more hydrophobic surface reduces the adsorption of sulphate species.

4. Materials and Methods

4.1. Materials

A cordierite ($2MgO.2Al_2O_3.5SiO_2$) monolith from Corning with 400 CPI was cut to obtain a mini-monolith (400 CPI, 1 cm diameter × 2.54 cm length; ~52 cells) with a mass of ~0.75 g. A colloidal suspension of γ-Al_2O_3 (25 wt.% Al_2O_3; average particle size 50 nm) provided by ULTRA

TEC Manufacturing, Inc. (Santa Ana, CA, USA) was used to prepare the washcoat. Pseudo boehmite, (γ-AlOOH, Sasol North America, Houston, TX, USA), product number is 23N4-80) with an average particle size of 90 nm was used as binding agent. $Ce(NO_3)_3.6H_2O$ (Aldrich 99% purity) and $Pd(NO_3)_2.xH_2O$ (Aldrich ≥ 99% purity, Oakville, Ontario, Canada) were used to prepare the aqueous solutions of Ce (2.5 wt.%) and Pd (0.42 wt.%) for sequential impregnation of the washcoated monolith.

4.2. Preparation of the Monolith Catalyst

Prior to use the γ-AlOOH was dried for 2 h at 120 °C and calcined in stagnant air, heating from room temperature to 350 °C at 10 °C/min and then holding the final temperature (350 °C) for 7 h. The γ-AlOOH (5 g) and 15 mL of H_2O were then added to the γ-Al_2O_3 colloidal solution (80 g) and stirred for an additional 1 h to obtain a suspension with 5 wt.% γ-AlOOH and 20 wt.% γ-Al_2O_3. As reported previously, γ-AlOOH improved the stability and uniformity of the washcoat [76]. The monolith was dried for 2 h at 120 °C prior to dip coating in the prepared suspension for 5 min. After removal from the suspension, pressurized air was used to remove any excess fluid trapped in the channels of the monolith. The washcoated monolith was subsequently dried for 2 h at 120 °C and calcined in stagnant air by heating from room temperature to 450 °C at 10 °C/min and then holding the final temperature for 7 h before cooling to room temperature. The dip coating was repeated to obtain the desired washcoat loading of ~27 wt.% on the monolith. The calcined and washcoated monolith was then wet impregnated with the Ce solution for 1 min, dried for 2 h at 120 °C and calcined in air flow of 100 cm^3(STP)·min^{-1} while heating from 25 to 450 °C at 10 °C/min and holding the final temperature for 15 h. The monolith was subsequently cooled to room temperature. Then, the washcoated monolith with CeO_2 was wet impregnated with the Pd solution for 1 min, dried for 2 h at 120 °C and calcined in air flow of 100 cm^3(STP) min^{-1} while heating from 25 to 450 °C at 10 °C/min and holding the final temperature for 15 h. The monolith was subsequently cooled to room temperature. For all monolith catalysts of this study, the nominal Pd loading was held constant at 0.5 wt.%. The final catalyst nominal compositions are reported in Table 5. For the Pd0Ce catalyst, after the washcoat was deposited on the monolith, the Pd was added according to the method already described, but without first adding the CeO_2.

Table 5. Nominal composition of monolith catalysts.

Sample	Catalyst Composition, wt.%				
	Pd	Ce	γ-AlOOH	γ-Al_2O_3	Cordierite
Pd0Ce	0.5	0	5.3	21.2	73.0
Pd1Ce	0.5	1.0	5.1	20.4	73.0
Pd2Ce	0.5	2.0	4.9	19.6	73.0
Pd4Ce	0.5	4.0	4.5	18.0	73.0

4.3. Monolith Characterization

The monolith catalyst BET (Brunauer-Emmett-Teller) surface area, pore volume and average pore size were determined from the N_2 adsorption-desorption isotherms measured at 77 K using a Micromeritics ASAP 2020 analyzer, (Micromeritics, Norcross, GA, USA). The monolith catalysts were crushed to a powder, dried at 110 °C under vacuum for 3 h to remove moisture prior to the analysis.

The monoliths were also analyzed using scanning electron microscopy (SEM) and Energy-dispersive X-ray spectroscopy (EDX). A JEOL JSM-5510 LV SEM (Jeol, St-Hubert, QC, Canada) was used to assess the surface morphology of the washcoated monolith. In the latter case, the monolith was sectioned to yield an internal channel for analysis. The presence of Ce and Pd in the analyzed zone was verified by EDX.

The sectioned monolith was also analyzed by X-ray photoelectron spectroscopy (XPS) to determine the properties of the surface of the washcoat. A Leybold MAX200 X-ray photoelectron spectrometer (XPS, Leybold, Export, PA, USA with Al Kα X-ray source was used for the analysis. A pass energy

of 192 eV was used for the survey scan and a pass energy of 48 eV was used for the narrow scan to determine the Pd oxidation state. XPSPEAK41 was used to analyze the spectra after background subtraction by the nonlinear Shirley method.

CO pulse chemisorption measurements were done using a Micromeritics AutoChemII 2920 analyzer (Micromeritics, Norcross, GA, USA). The powdered monolith catalyst was dried in an Ar flow at 200 °C for 2 h prior to being reduced in a 50 cm^3(STP) min^{-1} flow of 9.5 vol.% H_2/Ar (Praxair) at 100 °C for 1 h. After cooling to 50 °C in He the CO uptake was measured by passing pulses of 9.93 vol.% CO/He (Praxair) at 50 °C over the sample and measuring the CO adsorbed using a thermal conductivity detector (TCD). The catalyst reduction transformed the PdO to Pd^0, suitable for CO adsorption.

Ultrasonic vibration was used to evaluate the mechanical strength of the bond between the washcoat and the cordierite monolith [4]. A washcoated monolith was placed in an ultrasonic water bath (frequency 40 kHz) for 1 h. The sample was subsequently dried at 120 °C for 2 h and weighed. The weight loss of the washcoat following this treatment gave a relative measure of the adhesion of the washcoat to the cordierite monolith.

To assess the thermal stability of the washcoat, the same monolith was placed in an oven in air while heating to 1000 °C at 10 °C/min and holding the final temperature for 7 h. Subsequently, the monolith was subjected to the same ultrasonic vibration test as before, dried at 120 °C for 2 h and weighed to determine the mass loss.

4.4. Reaction System and Activity Measurements

The initial activity of the mini-monolith catalyst was measured by temperature-programmed reaction tests, herein referred to as temperature-programmed CH_4 oxidation tests (TPO), in a total feed gas flow of 1025 cm^3(STP)·min^{-1}, corresponding to a GHSV of 36,000 h^{-1}. The feed gas composition was 0.07 vol.% CH_4, 8.5 vol.% O_2, 0.06 vol.% CO, 8 vol.% CO_2 and 0, 2 or 5 vol.% H_2O in N_2 and He. Time-on-stream (TOS) tests were used to quantify the stability of the catalysts at 425 and 550 °C. For the TOS test the GHSV and feed gas composition was the same as the TPO, except the H_2O content was set at 10 vol.%. The chosen reaction conditions ensured the obtained CH_4 conversion data were not impacted by heat and mass transfer effects (see Suppementary Materials). Further details of the experimental set up have been reported previously [76].

5. Conclusions

A series of catalysts prepared on a ceramic cordierite monolith (400 CPI, 1 cm diameter × 2.54 cm length; ~52 cells), washcoated with different supports that contained CeO_2 and loaded with PdO, were evaluated for CH_4 oxidation. Adding CeO_2 did not have a significant impact on the adhesion and thermal stability of the washcoat. Adding CeO_2 to a PdO/γ-AlOOH/γ-Al_2O_3 washcoated monolith catalyst reduced the inhibition of CH_4 oxidation by H_2O at low temperature (<550 °C). The highest catalyst activity and stability for CH_4 oxidation in the presence of H_2O was obtained by adding 2 wt.% CeO_2 to the washcoat. Adding CeO_2 enhanced oxygen exchange with the active phase and reduced water adsorption on the catalyst, which led to improved activity and stability of the catalysts in the presence of H_2O. The results of this study confirmed the role of adding Ce to Pd based monolith catalyst to suppress the inhibition of the catalyst of CH_4 oxidation by H_2O and SO_2, as has been reported for powdered catalysts.

Supplementary Materials: The following are available online at http://www.mdpi.com/2073-4344/9/6/557/s1. XPS Pd 3d spectra measured for fresh and used catalysts. Time-on-stream data in 10 vol.% H_2O at 550 °C. Temperature-programmed oxidation profile for CO conversion as function of temperature for the catalysts. Mass and heat transfer calculations.

Author Contributions: Catalyst preparation, catalyst characterization and catalyst testing were done by Hamad Almohamadi under the direct supervision of K.J.S. Both authors contributed equally to the data analysis and manuscript preparation.

Funding: This research was funded by Westport Innovations Inc. and Natural Sciences and Engineering Research Council of Canada.

Acknowledgments: The financial support of Westport Innovations Inc. and the Natural Sciences and Engineering Research Council of Canada is gratefully acknowledged

Conflicts of Interest: The authors declare no conflict of interest.

References

1. Abbasi, R.; Huang, G.; Istratescu, G.M.; Wu, L.; Hayes, R.E. Methane oxidation over Pt, Pt: Pd, and Pd based catalysts: Effects of pre-treatment. *Can. J. Chem. Eng.* **2015**, *93*, 1474–1482. [CrossRef]
2. Gélin, P.; Primet, M. Complete oxidation of methane at low temperature over noble metal based catalysts: A review. *Appl. Catal. B Environ.* **2002**, *39*, 1–37. [CrossRef]
3. Ciuparu, D.; Lyubovsky, M.R.; Altman, E.; Pfefferle, L.D.; Datye, A. Catalytic combustion of methane over palladium-based catalysts. *Catal. Rev.* **2002**, *44*, 593–649. [CrossRef]
4. Adamowska, M.; Da Costa, P. Structured Pd/γ-Al_2O_3 Prepared by Washcoated Deposition on a Ceramic Honeycomb for Compressed Natural Gas Applications. *J. Nanoparticles* **2015**, *3*, 9–18. [CrossRef]
5. Choudhary, T.V.; Banerjee, S.; Choudhary, V.R. Catalysts for combustion of methane and lower alkanes. *Appl. Catal. A Gen.* **2002**, *234*, 1–23. [CrossRef]
6. Cargnello, M.; Jaén, J.J.D.; Garrido, J.C.H.; Bakhmutsky, K.; Montini, T.; Gámez, J.J.C.; Gorte, R.J.; Fornasiero, P. Exceptional Activity for Methane Combustion over Modular Pd@CeO_2 Subunits on Functionalized Al_2O_3. *Science* **2012**, *337*, 713–717. [CrossRef] [PubMed]
7. Zhu, G.; Han, J.; Zemlyanov, D.Y.; Ribeiro, F.H. The Turnover Rate for the Catalytic Combustion of Methane over Palladium Is Not Sensitive to the Structure of the Catalyst. *J. Am. Chem. Soc.* **2004**, *126*, 9896–9897. [CrossRef] [PubMed]
8. Hoyos, L.J.; Praliaud, H.; Primet, M. Catalytic combustion of methane over palladium supported on alumina and silica in presence of hydrogen sulfide. *Appl. Catal. A Gen.* **1993**, *98*, 125–138. [CrossRef]
9. Lampert, J.K.; Kazi, M.S.; Farrauto, R.J. Palladium catalyst performance for methane emissions abatement from lean burn natural gas vehicles. *Appl. Catal. B Environ.* **1997**, *14*, 211–223. [CrossRef]
10. Gholami, R.; Alyani, M.; Smith, K.J. Deactivation of Pd Catalysts by Water during Low Temperature Methane Oxidation Relevant to Natural Gas Vehicle Converters. *Catalysts* **2015**, *5*, 561. [CrossRef]
11. Mowery, D.L.; McCormick, R.L. Deactivation of alumina supported and unsupported PdO methane oxidation catalyst: The effect of water on sulfate poisoning. *Appl. Catal. B Environ.* **2001**, *34*, 287–297. [CrossRef]
12. Li, Z.; Hoflund, G.B. A review on complete oxidation of methane at low temperatures. *J. Nat. Gas Chem.* **2003**, *12*, 153–160.
13. Gandhi, H.S.; Graham, G.W.; McCabe, R.W. Automotive exhaust catalysis. *J. Catal.* **2003**, *216*, 433–442. [CrossRef]
14. Narui, K.; Furuta, K.; Yata, H.; Nishida, A.; Kohtoku, Y.; Matsuzaki, T. Catalytic activity of PdO/ZrO_2 catalyst for methane combustion. *Catal. Today* **1998**, *45*, 173–178. [CrossRef]
15. Farrauto, R.J.; Lampert, J.K.; Hobson, M.C.; Waterman, E.M. Thermal decomposition and reformation of PdO catalysts; support effects. *Appl. Catal. B Environ.* **1995**, *6*, 263–270. [CrossRef]
16. Haneda, M.; Mizushima, T.; Kakuta, N.; Ueno, A.; Sato, Y.; Matsuura, S.; Kasahara, K.; Sato, M. Structural Characterization and Catalytic Behavior of Al_2O_3-Supported Cerium Oxides. *Bull. Chem. Soc. Jpn.* **1993**, *66*, 1279–1288. [CrossRef]
17. Park, J.; Cho, J.H.; Kim, Y.J.; Kim, E.S.; Han, H.S.; Shin, C. Hydrothermal stability of Pd/ZrO_2 catalysts for high temperature methane combustion. *Appl. Catal. B Environ.* **2014**, *160*, 135–143. [CrossRef]
18. Colussi, S.; Trovarelli, A.; Cristiani, C.; Lietti, L.; Groppi, G. The influence of ceria and other rare earth promoters on palladium-based methane combustion catalysts. *Catal. Today* **2012**, *180*, 124–130. [CrossRef]
19. Ramírez-López, R.; Elizalde-Martinez, I.; Balderas-Tapia, L. Complete catalytic oxidation of methane over Pd/CeO_2–Al_2O_3: The influence of different ceria loading. *Catal. Today* **2010**, *150*, 358–362. [CrossRef]
20. Stasinska, B.; Gac, W.; Ioannides, T.; Machocki, A. Complete oxidation of methane over palladium supported on alumina modified with calcium, lanthanum, and cerium ions. *J. Nat. Gas Chem.* **2007**, *16*, 342–348. [CrossRef]

21. Groppi, G.; Cristiani, C.; Lietti, L.; Ramella, C.; Valentini, M.; Forzatti, P. Effect of ceria on palladium supported catalysts for high temperature combustion of CH4 under lean conditions. *Catal. Today* **1999**, *50*, 399–412. [CrossRef]
22. Fan, X.; Wang, F.; Zhu, T.; He, H. Effects of Ce on catalytic combustion of methane over Pd-Pt/Al_2O_3 catalyst. *J. Environ. Sci.* **2012**, *24*, 507–511. [CrossRef]
23. Persson, K.; Ersson, A.; Colussi, S.; Trovarelli, A.; Järås, S.G. Catalytic combustion of methane over bimetallic Pd–Pt catalysts: The influence of support materials. *Appl. Catal. B Environ.* **2006**, *66*, 175–185. [CrossRef]
24. Ciuparu, D.; Perkins, E.; Pfefferle, L. In situ DR-FTIR investigation of surface hydroxyls on γ-Al_2O_3 supported PdO catalysts during methane combustion. *Appl. Catal. A Gen.* **2004**, *263*, 145–153. [CrossRef]
25. Colussi, S.; Gayen, A.; Farnesi Camellone, M.; Boaro, M.; Llorca, J.; Fabris, S.; Trovarelli, A. Nanofaceted Pd-O Sites in Pd-Ce Surface Superstructures: Enhanced Activity in Catalytic Combustion of Methane. *Angew. Chem. Int. Ed.* **2009**, *48*, 8481–8484. [CrossRef] [PubMed]
26. Escandón, L.S.; Niño, D.; Díaz, E.; Ordóñez, S.; Díez, F.V. Effect of hydrothermal ageing on the performance of Ce-promoted PdO/ZrO_2 for methane combustion. *Catal. Commun.* **2008**, *9*, 2291–2296. [CrossRef]
27. Burch, R.; Loader, P.K.; Urbano, F.J. 1st World Conference Environmental Catalysis for a Better World and Life Some aspects of hydrocarbon activation on platinum group metal combustion catalysts. *Catal. Today* **1996**, *27*, 243–248. [CrossRef]
28. Gélin, P.; Urfels, L.; Primet, M.; Tena, E. Complete oxidation of methane at low temperature over Pt and Pd catalysts for the abatement of lean-burn natural gas fuelled vehicles emissions: Influence of water and sulphur containing compounds. *Catal. Today* **2003**, *83*, 45–57. [CrossRef]
29. Alyani, M.; Smith, K.J. A kinetic analysis of the inhibition of CH_4 oxidation by H_2O on PdO/Al_2O_3 and CeO_2/PdO/Al_2O_3 catalysts. *Ind Eng Chem Res* **2016**, *55*, 8309–8318. [CrossRef]
30. Gomathi, A.; Vickers, S.M.; Gholami, R.; Alyani, M.; Man, R.W.; MacLachlan, M.J.; Smith, K.J.; Wolf, M.O. Nanostructured Materials Prepared by Surface-Assisted Reduction: New Catalysts for Methane Oxidation. *Acs Appl. Mater. Interfaces* **2015**, *7*, 19268–19273. [CrossRef]
31. Toso, A.; Colussi, S.; Llorca, J.; Trovarelli, A. The dynamics of PdO-Pd phase transformation in the presence of water over Si-doped Pd/CeO_2 methane oxidation catalysts. *Appl. Catal. A Gen.* **2019**, *574*, 79–86. [CrossRef]
32. Vergunst, T.; Kapteijn, F.; Moulijn, J.A. Monolithic catalysts — non-uniform active phase distribution by impregnation. *Appl. Catal. A Gen.* **2001**, *213*, 179–187. [CrossRef]
33. Geus, J.W.; Van Giezen, J.C. Monoliths in catalytic oxidation. *Catal. Today* **1999**, *47*, 169–180. [CrossRef]
34. Nijhuis, T.A.; Beers, A.E.W.; Vergunst, T.; Hoek, I.; Kapteijn, F.; Moulijn, J.A. Preparation of monolithic catalysts. *Catal. Rev. Sci. Eng.* **2001**, *43*, 345–380. [CrossRef]
35. Hayes, R.E.; Awdry, S.; Kolaczkowski, S.T. Catalytic combustion of methane in a monolith washcoat: Effect of water inhibition on the effectiveness factor. *Can. J. Chem. Eng.* **1999**, *77*, 688–697. [CrossRef]
36. Thevenin, P.O.; Menon, P.G.; Järås, S.G. Catalytic Total Oxidation of Methane. Part II. Catalytic Processes to Convert Methane: Partial or Total Oxidation. *CATTECH* **2003**, *7*, 10–22. [CrossRef]
37. Govender, S.; Friedrich, H.B. Monoliths: A Review of the Basics, Preparation Methods and Their Relevance to Oxidation. *Catalysts* **2017**, *7*, 62. [CrossRef]
38. Kucharczyk, B.; Tylus, W.; Kępiński, L. Pd-based monolithic catalysts on metal supports for catalytic combustion of methane. *Appl. Catal. B Environ.* **2004**, *49*, 27–37. [CrossRef]
39. Ordóñez, S.; Hurtado, P.; Sastre, H.; Díez, F.V. Methane catalytic combustion over Pd/Al2O3 in presence of sulphur dioxide: Development of a deactivation model. *Appl. Catal. A Gen.* **2004**, *259*, 41–48. [CrossRef]
40. Kikuchi, R.; Maeda, S.; Sasaki, K.; Wennerström, S.; Eguchi, K. Low-temperature methane oxidation over oxide-supported Pd catalysts: Inhibitory effect of water vapor. *Appl. Catal. A Gen.* **2002**, *232*, 23–28. [CrossRef]
41. Persson, K.; Pfefferle, L.D.; Schwartz, W.; Ersson, A.; Järås, S.G. Stability of palladium-based catalysts during catalytic combustion of methane: The influence of water. *Appl. Catal. B Environ.* **2007**, *74*, 242–250. [CrossRef]
42. Zhu, G.; Han, J.; Zemlyanov, D.Y.; Ribeiro, F.H. Temperature dependence of the kinetics for the complete oxidation of methane on palladium and palladium oxide. *J. Phys. Chem. B* **2005**, *109*, 2331–2337. [CrossRef] [PubMed]
43. Stasinska, B.; Machocki, A.; Antoniak, K.; Rotko, M.; Figueiredo, J.L.; Gonçalves, F. Importance of palladium dispersion in Pd/Al_2O_3 catalysts for complete oxidation of humid low-methane–air mixtures. *Catal. Today* **2008**, *137*, 329–334. [CrossRef]

44. Roth, D.; Gélin, P.; Primet, M.; Tena, E. Catalytic behaviour of Cl-free and Cl-containing Pd/Al_2O_3 catalysts in the total oxidation of methane at low temperature. *Appl. Catal. A Gen.* **2000**, *203*, 37–45. [CrossRef]
45. Burch, R.; Urbano, F.; Loader, P. Methane combustion over palladium catalysts: The effect of carbon dioxide and water on activity. *Appl. Catal. A Gen.* **1995**, *123*, 173–184. [CrossRef]
46. Burch, R. Low NO_x options in catalytic combustion and emission control. *Catal. Today* **1997**, *35*, 27–36. [CrossRef]
47. Lucena, P.; Vadillo, J.M.; Laserna, J.J. Mapping of platinum group metals in automotive exhaust three-way catalysts using laser-induced breakdown spectrometry. *Anal. Chem.* **1999**, *71*, 4385–4391. [CrossRef]
48. Muraki, H.; Shinjoh, H.; Fujitani, Y. Effect of lanthanum on the no reduction over palladium catalysts. *Appl. Catal.* **1986**, *22*, 325–335. [CrossRef]
49. Wang, J.; Chen, H.; Hu, Z.; Yao, M.; Li, Y. A review on the Pd-based three-way catalyst. *Catal. Rev.* **2015**, *57*, 79–144. [CrossRef]
50. Di Monte, R.; Fornasiero, P.; Kašpar, J.; Graziani, M.; Gatica, J.; Bernal, S.; Gómez-Herrero, A. Stabilisation of nanostructured Ce_0. $2Zr_0$. $8O_2$ solid solution by impregnation on Al_2O_3: A suitable method for the production of thermally stable oxygen storage/release promoters for three-way catalysts. *Chem. Commun.* **2000**, 2167–2168. [CrossRef]
51. Yao, H.; Yao, Y.Y. Ceria in automotive exhaust catalysts: I. Oxygen storage. *J. Catal.* **1984**, *86*, 254–265. [CrossRef]
52. Su, E.; Montreuil, C.; Rothschild, W. Oxygen storage capacity of monolith three-way catalysts. *Appl. Catal.* **1985**, *17*, 75–86. [CrossRef]
53. Hailstone, R.; DiFrancesco, A.; Leong, J.; Allston, T.; Reed, K. A study of lattice expansion in CeO_2 nanoparticles by transmission electron microscopy. *J. Phys. Chem. C* **2009**, *113*, 15155–15159. [CrossRef]
54. Ozawa, M.; Kimura, M. Effect of cerium addition on the thermal stability of gamma alumina support. *J. Mater. Sci. Lett.* **1990**, *9*, 291–293. [CrossRef]
55. Piras, A.; Trovarelli, A.; Dolcetti, G. Remarkable stabilization of transition alumina operated by ceria under reducing and redox conditions. *Appl. Catal. B Environ.* **2000**, *28*, L77–L81. [CrossRef]
56. Jiang, P.; Lu, G.; Guo, Y.; Guo, Y.; Zhang, S.; Wang, X. Preparation and properties of a γ-Al_2O_3 washcoat deposited on a ceramic honeycomb. *Surf. Coat. Technol.* **2005**, *190*, 314–320. [CrossRef]
57. Moulder, J.F. *Handbook of X-Ray Photoelectron Spectroscopy*; National Institute of Informatics: Tokyo, Japan, 1995; pp. 230–232.
58. Cullis, C.; Willatt, B. Oxidation of methane over supported precious metal catalysts. *J. Catal.* **1983**, *83*, 267–285. [CrossRef]
59. Haneda, M.; Mizushima, T.; Kakuta, N. Synergistic effect between Pd and nonstoichiometric cerium oxide for oxygen activation in methane oxidation. *J. Phys. Chem. B* **1998**, *102*, 6579–6587. [CrossRef]
60. Colussi, S.; Trovarelli, A.; Vesselli, E.; Baraldi, A.; Comelli, G.; Groppi, G.; Llorca, J. Structure and morphology of Pd/Al_2O_3 and $Pd/CeO_2/Al_2O_3$ combustion catalysts in Pd–PdO transformation hysteresis. *Appl. Catal. A Gen.* **2010**, *390*, 1–10. [CrossRef]
61. Fouladvand, S.; Schernich, S.; Libuda, J.; Grönbeck, H.; Pingel, T.; Olsson, E.; Skoglundh, M.; Carlsson, P. Methane oxidation over Pd supported on ceria–alumina under rich/lean cycling conditions. *Top. Catal.* **2013**, *56*, 410–415. [CrossRef]
62. Fujimoto, K.; Ribeiro, F.H.; Avalos-Borja, M.; Iglesia, E. Structure and reactivity of PdO_x/ZrO_2 catalysts for methane oxidation at low temperatures. *J. Catal.* **1998**, *179*, 431–442. [CrossRef]
63. Yao, Y.Y. Oxidation of alkanes over noble metal catalysts. *Ind. Eng. Chem. Prod. Res. Dev.* **1980**, *19*, 293–298. [CrossRef]
64. Oh, S.H.; Mitchell, P.J.; Siewert, R.M. Methane oxidation over alumina-supported noble metal catalysts with and without cerium additives. *J. Catal.* **1991**, *132*, 287–301. [CrossRef]
65. Xiao, L.; Sun, K.; Xu, X.; Li, X. Low-temperature catalytic combustion of methane over Pd/CeO_2 prepared by deposition–precipitation method. *Catal. Commun.* **2005**, *6*, 796–801. [CrossRef]
66. Schwartz, W.R.; Ciuparu, D.; Pfefferle, L.D. Combustion of Methane over palladium-based catalysts: Catalytic deactivation and Role of the Support. *J. Phys. Chem. C* **2012**, *116*, 8587–8593. [CrossRef]
67. Farrauto, R.J.; Hobson, M.; Kennelly, T.; Waterman, E. Catalytic chemistry of supported palladium for combustion of methane. *Appl. Catal. A Gen.* **1992**, *81*, 227–237. [CrossRef]

68. Shyu, J.; Otto, K.; Watkins, W.; Graham, G.; Belitz, R.; Gandhi, H. Characterization of Pd/γ-alumina catalysts containing ceria. *J. Catal.* **1988**, *114*, 23–33. [CrossRef]
69. Colussi, S.; Trovarelli, A.; Groppi, G.; Llorca, J. The effect of CeO_2 on the dynamics of Pd–PdO transformation over Pd/Al_2O_3 combustion catalysts. *Catal. Commun.* **2007**, *8*, 1263–1266. [CrossRef]
70. Cullis, C.; Nevell, T.; Trimm, D. Role of the catalyst support in the oxidation of methane over palladium. *J. Chem. Soc. Faraday Trans. Phys. Chem. Condens. Phases* **1972**, *68*, 1406–1412. [CrossRef]
71. Araya, P.; Guerrero, S.; Robertson, J.; Gracia, F.J. Methane combustion over Pd/SiO_2 catalysts with different degrees of hydrophobicity. *Appl. Catal. A Gen.* **2005**, *283*, 225–233. [CrossRef]
72. Okumura, K.; Shinohara, E.; Niwa, M. Pd loaded on high silica beta support active for the total oxidation of diluted methane in the presence of water vapor. *Catal. Today* **2006**, *117*, 577–583. [CrossRef]
73. Ruiz, J.A.; Fraga, M.A.; Pastore, H.O. Methane combustion over Pd supported on MCM-41. *Appl. Catal. B Environ.* **2007**, *76*, 115–122. [CrossRef]
74. Carchini, G.; García-Melchor, M.; Łodziana, Z.; López, N. Understanding and tuning the intrinsic hydrophobicity of rare-earth oxides: A DFT U study. *Acs Appl. Mater. Interfaces* **2015**, *8*, 152–160. [CrossRef] [PubMed]
75. Honkanen, M.; Wang, J.; Kärkkäinen, M.; Huuhtanen, M.; Jiang, H.; Kallinen, K.; Keiski, R.L.; Akola, J.; Vippola, M. Regeneration of sulfur-poisoned Pd-based catalyst for natural gas oxidation. *J. Catal.* **2018**, *358*, 253–265. [CrossRef]
76. Almohamadi, H.; Smith, K.J. Beneficial Effect of Adding g-AlOOH to the g-Al_2O_3 Washcoat of a PdO Catalyst for Methane Oxidation. *Can. J. Chem. Eng.* **2019**. accepted.